



Cite this: RSC Adv., 2017, 7, 19353

## Highly sensitive electrochemical determination of captopril using CuO modified ITO electrode: the effect of *in situ* grown nanostructures over signal sensitivity†

Razium Ali Soomro, <sup>a</sup> Mawada Mohamed Tunesi, <sup>b</sup> Selcan Karakus<sup>b</sup> and Nazar Kalwar<sup>a</sup>

The study describes a new approach for the direct electro-oxidation of captopril (CAP) drug using a CuO modified ITO electrode. The modified ITO electrode consists of an *in situ* grown film which accommodates dense CuO nanostructures with morphological features similar to flowers. The *in situ* growth over the ITO substrate was achieved using a simple hydrothermal route with the assistance of malonic acid which acted as an effective growth template. The devised electrode was evaluated in reference to its slurry-derived counterpart which involved surface modification of GCE using a conventional approach (drop-casting). The competitive evaluation of the discussed electrodes against the electro-oxidation of CAP, provided significant evidence to support the importance of controlled nanostructure distribution over the electrode surface to achieve higher signal sensitivity and reproducibility. The devised ITO/CuO electrode was known to possess excellent sensing capability against CAP within the linear working range of 0.01 to 3.43  $\mu$ M with signal sensitivity down to  $2 \times 10^{-3}$   $\mu$ M. Moreover, the ITO/CuO was noted to exhibit high charge transfer co-efficient ( $\alpha$ ), diffusion co-efficient ( $D$ ) and rate constant values of 0.83,  $9.28 \times 10^{-5}$   $\text{cm}^2 \text{ s}^{-1}$  and  $3.5 \times 10^3$   $\text{mol}^{-1} \text{ L s}^{-1}$  respectively. In addition, the successful usage of ITO/CuO for CAP determination from commercial tablets and human urine samples further indicated the practical workability of the proposed electrode system.

Received 6th February 2017

Accepted 27th March 2017

DOI: 10.1039/c7ra01538k

rsc.li/rsc-advances

### 1. Introduction

The accurate analysis of biological and environmentally important molecules is a crucial task due to their clinical and toxicological significance.<sup>1,2</sup> The conventional strategies which include techniques such as LC-MS,<sup>5</sup> UV-spectrophotometry,<sup>6</sup> HPLC<sup>7</sup> and GC,<sup>8</sup> despite their high sensitivity and accuracy are not only time-consuming, but are also accompanied by complex sample preparation and analysis protocols. Moreover, the lab-based practice of such techniques classify them as unsuitable candidates for the widespread range of analytical applications.<sup>3,4</sup> In contrast, the electrochemical approach coupled with nano-materials ensure a promising avenue for the production of simpler, sensitive and cost-effective sensor systems with the potential for on-site detection.<sup>3,5,6</sup> The integration of nano-materials with the electrochemical approach can drastically enhance the characteristic properties of the conventional

electrodes, thus, enabling sensitive and selective quantification of numerous clinical and toxicologically important molecules.<sup>7-9</sup>

The most convenient and widely practiced method for the modification of conventional electrodes (Au, Pt and Ag) involves simple drop casting/pasting of nanomaterials over the surface of pre-polished electrode.<sup>10</sup> Despite the effectiveness of method, the said approach prevents the controlled distribution of nanostructures over the surface of electrode effecting both the available active sites and the electrochemical performance of electrode. In addition, the use of polymeric binders to restrict the abrasion of the deposited layer further hinders the analyte diffusion process at the electrode-solution interface.<sup>11</sup> Although, various combinations of nanomaterials have been reported promising towards the achievement of higher signal sensitivity.<sup>12</sup> However, this conventional off-substrate strategy for the electrode modification results in strong signal fluctuations, poor surface coverage and smaller signal reproducibility. To overcome such issues, research focus has been shifted towards the *in situ* growth of nanomaterials over the flexible yet conductive substrates which later can be considered as working electrode for the sensor development. The *in situ* growth of nanostructures over electrode surface can radically improve the control of morphology, arrangement and surface coverage of

<sup>a</sup>National Centre of Excellence in Analytical Chemistry, University of Sindh, Jamshoro, 76080, Pakistan. E-mail: raziumsoomro@gmail.com; Fax: +92 22 9213431; Tel: +92 3332761963

<sup>b</sup>Department of Chemistry, Istanbul University, Avcilar 34320, Istanbul, Turkey

† Electronic supplementary information (ESI) available. See DOI: 10.1039/c7ra01538k



nanostructures. Moreover, the binder-less strategy can significantly increase the electrode-modifier contact points which would ultimately contribute towards high electron-transfer kinetics and signal sensitivity. Recently, Wang T., *et al.* (2016)<sup>13</sup> described the working capability of *in situ* grown CuO nanostructures for the direct electro-oxidation of glucose. Similarly, graphene-encapsulated gold nanoparticle have also been suggested for the direct electro-oxidation of glucose.<sup>14</sup> Thus, despite the excessive usage of ITO, the usage of such flexible substrates in the area of electrode based sensor system is much less-explored.

Captopril (CAP), chemically known as [2S-1-(3-mercaptopro-2-methyl-propionyl)-L-proline] is a widely used antihypertensive drug. It is known for its relief from hypertension and congestive heart failure. Besides this, CAP is also prescribed for problems such angina, Raynaud's phenomenon and rheumatoid arthritis. To date, various electrochemical approaches involving numerous redox mediators such as nano-TiO<sub>2</sub>/ferrocene carboxylic acid, multiwall carbon nanotubes, and chlorpromazine<sup>15,16</sup> have been considered for the sensitive quantification of CAP. In a recent effort, CuO nanoparticles/multi-wall carbon nanotube and Cu(II) ions modified electrodes have been reported sufficiently effective for the direct electro-oxidation of CAP based on the affinity between the electrode modifier and thiol functionality associated with CAP molecules.<sup>17,18</sup> Thus, in continuation of our previous work,<sup>17</sup> the present study discusses the influence of *in situ* grown CuO nanostructures on the signal sensitivity measured for the direct electro-oxidation of CAP in aqueous medium. The discussed approach in reference to the conventional off-substrate strategy (drop casting) provides sufficient evidence for the achievement of high signal sensitivity, extreme reproducibility and long-lasting competency of the developed electrode. Moreover, the successful quantification of CAP from the commercial tablets and human urine samples further reflected the practical applicability of the proposed electrode.

## 2. Experiment

### 2.1 Chemicals and reagents

Analytical grade copper chloride (CuCl<sub>2</sub>·2H<sub>2</sub>O), malonic acid (C<sub>3</sub>H<sub>4</sub>O<sub>4</sub>) ammonia solution (NH<sub>3</sub>) 35% and Britton–Robinson buffer (BRB) (0.1 M) purchased from Sigma Aldrich (Germany). Captopril (99.0%), glucose (C<sub>6</sub>H<sub>12</sub>O<sub>6</sub>), uric acid (C<sub>5</sub>H<sub>4</sub>N<sub>4</sub>O<sub>3</sub>), vitamin C (C<sub>6</sub>H<sub>8</sub>O<sub>6</sub>) potassium chloride (KCl), magnesium chloride (MgCl<sub>2</sub>), aluminum chloride (AlCl<sub>3</sub>), sodium nitrate (NaNO<sub>3</sub>) were also obtained from Sigma Chemicals (USA). Nafion® solution (C<sub>7</sub>HF<sub>13</sub>O<sub>5</sub>S·C<sub>2</sub>F<sub>4</sub>) was purchased from Merck chemicals (shanghai) co. ltd.

### 2.2 The *in situ* growth of CuO nanostructures over ITO substrate

The *in situ* growth of CuO nanostructures was achieved using modified hydrothermal method with the assistance of malonic acid taken as effective growth template. In a typical experiment, 1.63 g of CuCl<sub>2</sub>·5H<sub>2</sub>O was allowed to vortex with 0.7 g of malonic acid in 100 mL of de-ionised water. After complete

homogenisation, the pre-cleaned ITO slides (1 × 1 cm<sup>2</sup>) were introduced within the container with their conductive sides directed upwards. To ensure proper electrical connections, a small portion of the inserted slide was covered with paper tape, which was later removed for electrical measurement. The mixture was then introduced 5 mL of ammonia solution (35%) to the initiate nucleation process. The container was then sealed with aluminum foil and placed in a pre-heated electric oven at 80 °C for 9 h of hydrothermal treatment. At the completion of growth process, the ITO slides were separated from the mixture and thoroughly rinsed with de-ionised water and ethanol to remove any surface bound impurities.

### 2.3 The characterisation and electrochemical assessment of the developed electrode

The *in situ* grown CuO nanostructures was characterised using high resolution scanning electron microscopy (HR-SEM) (JEOL JSM-7001F) (Japan) installed with energy dispersive spectroscopy (EDS) (Oxford) system and X-ray diffraction (XRD) (Bruker D-8) (Germany). The electrochemical behavior of the devised electrode was assessed using bipotentiostat (E-760) (CH Instruments) (USA) with an electrochemical cell housing three electrodes. The standard Ag/AgCl and platinum wire was taken as reference and auxiliary electrodes respectively. The modified ITO based electrode was connected as a working electrode. To fully understand the influence of *in situ* grown nanostructures on the generated electro-oxidation signal. The electrochemical behavior of ITO based electrode was assessed in reference to GCE which was modified with the powdered version of the as-synthesised nanostructures using the conventional drop casting methodology. The modification of GCE was attained by depositing a pre-formed suspension (0.2 mg into 1 mL of methanol) of as-synthesised CuO nanostructure powder directly over the surface of pre-polished GCE. The modified surface was then covered with 1.5 µL of Nafion® and dried under ambient air condition. The discussed electrodes have been identified as ITO/CuO and GCE/CuO throughout the manuscript respectively.

### 2.4 The real samples

The CAP tablets with declared amount of 25 mg were purchased from the local pharmacy for the quantitative examination. The tablets were grounded and homogenised in BRB solution of 0.1 M with pH of 4.5 to produce final solution of 0.1 µM (CAP) prior to analysis. The standard addition method was further considered to validate the quantification of CAP from human urine samples which were collected from healthy volunteers against an informed consent. The collected urine samples were stored in refrigerator at 4 °C and were diluted prior analysis.

## 3. Results and discussion

### 3.1 The characterisation of *in situ* grown CuO nanostructures

Fig. 1 shows the HR-SEM images of ITO substrate with *in situ* grown CuO nanostructures. As seen, the formed nanostructures are densely populated with flower-like morphological features



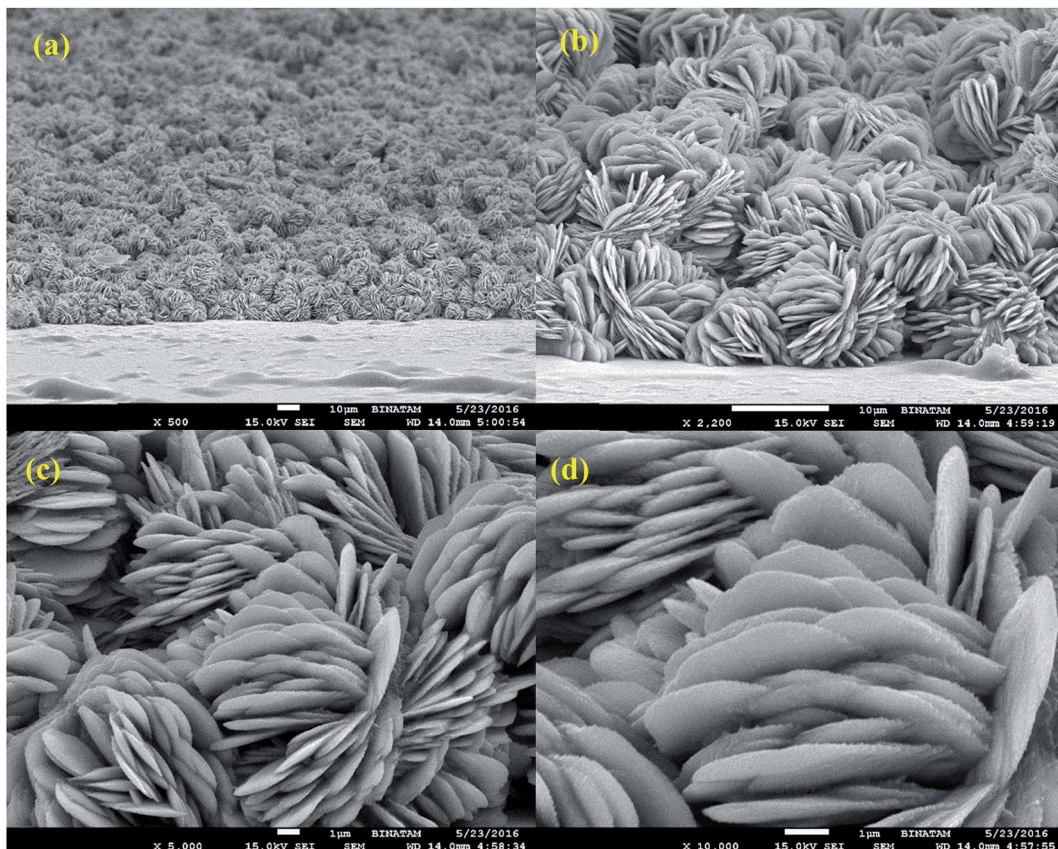


Fig. 1 HR-SEM images of *in situ* grown CuO nanostructures over ITO substrate.

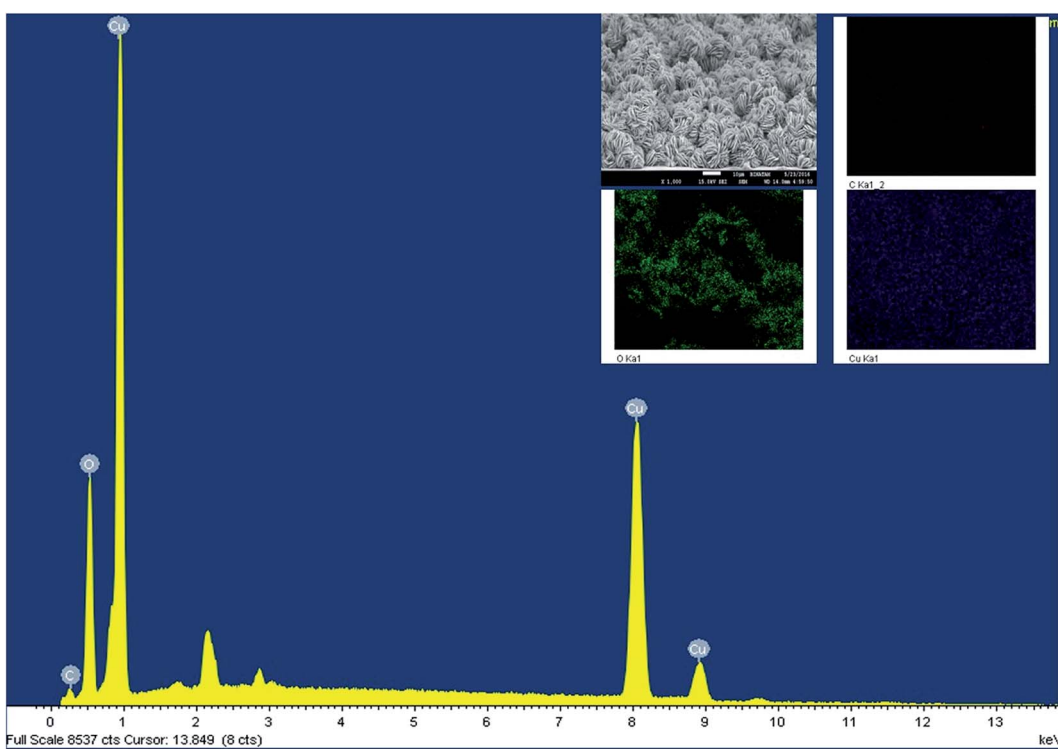


Fig. 2 The EDX spectra for *in situ* grown CuO nanostructures with elemental mapping shown as inset figure.

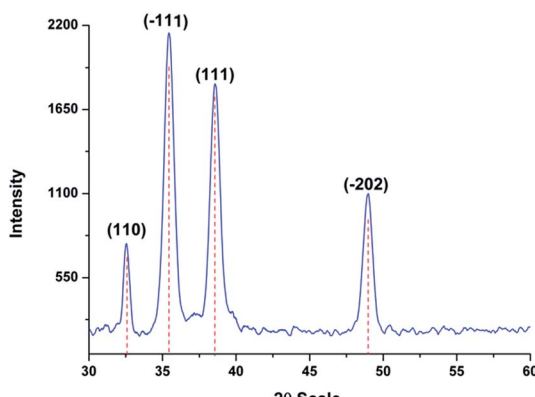


Fig. 3 XRD for the *in situ* grown CuO nanostructures over ITO substrate.

which are composed of interconnected thin flakes. Unlike, the other studies where smooth surface edges have been observed for flower shaped nanostructures. In this case, the *in situ* grown flakes possess teeth-like sharp edges (Fig. 1(d)). To ensure versatility of the proposed approach, a similar sample was prepared without the application of malonic acid. The captured

SEM image (Fig. S1†) is evident of growing bulky CuO material without any proper structural or morphological characteristics. More importantly, the formed thick layer had negligibly adherence to the underlying ITO substrate and thus, transformed into dust when subjected to drying. Hence, it can be stated that the utilised template plays an important role both as modifier and adhesive to promote the *in situ* growth of CuO nanostructures over ITO substrate. The *in situ* grown flakes had an estimated thickness of 10–20 nm with average of  $5 \pm 3.5$  nm noted for the teeth-like feature. To ensure no external impurities resides over the formed nanostructures, EDX analysis was carried for the representative sample. As seen, the EDX spectra consists of no peaks other than copper and oxygen (Fig. 2(a)). The XRD pattern recorded for ITO/CuO is shown in Fig. 3. The pattern displays sharp peaks indexed to (110), (111), (-111), (-202) planes of the monoclinic CuO as standardised against ICCD card no. 80-0076.<sup>19</sup> The absence of any irrelevant peaks in the XRD pattern further signifies the chemical purity of the formed product. The digital image for the obtained ITO slides is shown in Fig. S2.†

In case of *in situ* growth, slow and controlled precipitation is highly describable to achieve steady and controlled growth over the ITO surface. In case of NH<sub>3</sub>, the hydroxyl (OH<sup>-</sup>) ions are

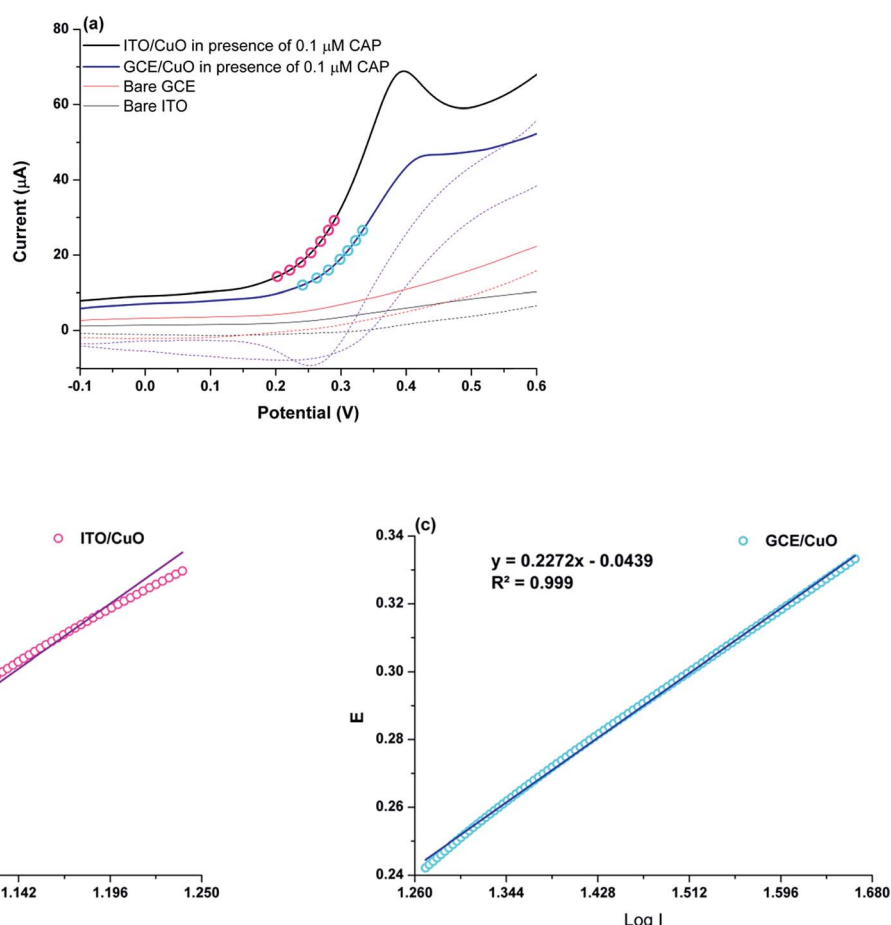


Fig. 4 (a) CV response for ITO/CuO and GCE/CuO against 0.1  $\mu$ M CAP (b) and (c) shows the corresponding Tafel slopes obtained from the raising portion of the recorded voltammograms.



Table 1 Analytical characteristics of the ITO/CuO sensor in comparison with various electrode based sensor systems for CAP quantification

Electrode	Modifier	LOD (M)	LDR (M)	Electron transfer coefficient ( $D$ )	Diffusion coefficient $\text{cm}^2 \text{s}^{-1}$	Rate constant of the catalytic process $(k_h) \text{ mol}^{-1} \text{L s}^{-1}$	Reference
Carbon paste electrodes	CuO NPs/MWCNTs-CPE	$2.9 \times 10^{-7}$	$4.6 \times 10^{-7}$ – $1.0 \times 10^{-5}$	0.43	$2.1 \times 10^{-7}$	$1.449 \times 10^5$	18
Carbon paste electrode	NiO/NPs/DED/CPE	$7.0 \times 10^{-9}$	$3.5 \times 10^{-8}$ – $5.5 \times 10^{-4}$	0.72	$2.9 \times 10^{-5}$	$1.49 \times 10^3$	22
Carbon paste electrode	Si/Al-APTMS-BPK-Mn	$9.0 \times 10^{-8}$	$3.0 \times 10^{-7}$ – $300 \times 10^{-4}$	0.69	$1.55 \times 10^{-4}$	$6.21 \times 10^2$	23
Carbon paste electrodes	2CBFZCCPE	$9 \times 10^{-8}$	$5.0 \times 10^{-7}$ – $9.0 \times 10^{-4}$	0.64	$1.2 \times 10^{-6}$	$8.9 \times 10^3$	24
ITO electrode	CuO	$2.0 \times 10^{-9}$	$1.0 \times 10^{-8}$ – $3.43 \times 10^{-6}$	0.83	$9.28 \times 10^{-5}$	$3.5 \times 10^3$	This work

considered responsible for the generation of metal hydroxide  $\text{Cu}(\text{OH})_2$  nuclei as the consequence of metal–ammonia complex dissociation (eqn (ii)). The use of malonic acid as sacrificial template further reduces the said precipitation, allowing *in situ* growth of CuO nuclei over conductive ITO substrate. The use of malonic acid also ensure directional growth of nuclei which then leads to the formation of regular nanostructures interconnected with sharp flake-like structural features.

The growth process can be described using the following set of equations:



Unlike NiO and  $\text{Co}_3\text{O}_4$  which necessitate high temperature to convert from hydroxide to oxide phase, CuO can easily transform from  $\text{Cu}(\text{OH})_2$  (orthorhombic) to CuO (monoclinic) at low temperatures of 85 °C. This in addition to the provision of added surface support from ITO substrate further decrease the surface effects resulting in the preservation of the characteristic properties of the synthesised CuO nanostructures.<sup>20</sup>

### 3.2 The electrochemical oxidation of CAP over modified ITO electrode

To ascertain the potential of ITO/CuO for the electro-oxidation of CAP, the developed electrode was tested in 0.1 μM of CAP

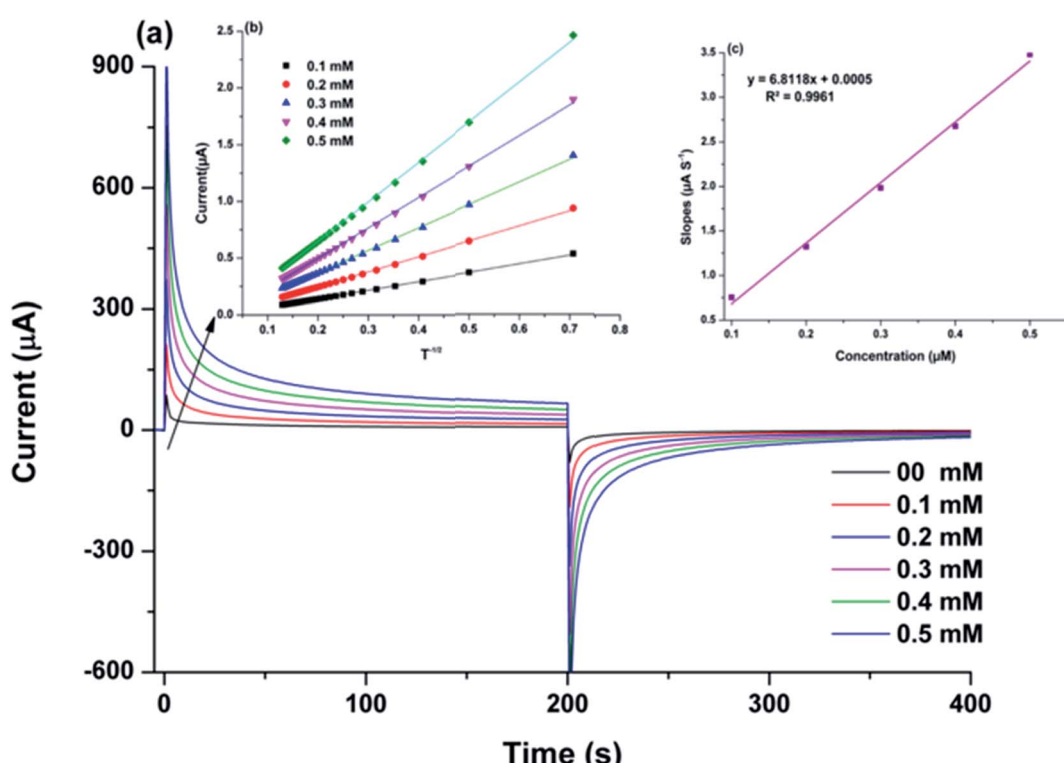


Fig. 5 (a) Chronoamperometric measurement recorded for ITO/CuO against CAP in concentration range of 0.1 to 0.5 mM (b) linear fit data for current vs.  $t^{-1/2}$  and (b) plot of corresponding slopes against the utilised concentration of CAP.



within 0.1 M BRB (pH 4.5). The measurements were carried in reference to bare ITO, GCE and CGE modified with the powdered version of the as-synthesised nanostructures. As seen, the response of ITO/CuO is relatively higher in current density with lower potential values compared to its other competitors (Fig. 4(a)). Besides this, the anodic peak shape largely differ in both cases. Since, the type of nanostructures used in the electrode modification process are exactly similar, the variation in the anodic peak characteristic can only be attributed to the distribution and coverage of nanostructures over the surface of electrodes. As observed from SEM images, the ITO/CuO exhibits complete coverage of the electrode surface area with negligible pin-hole formation. The proposed *in situ* growth strategy offer direct growth of regularly arranged CuO nanostructures with increased number of contact-points between the electro-active material and conductive substrate.<sup>14</sup> Thus, enabling high signal reproducibility based on their identical surface-analyte interactions. Contrary to this, the direct modification of GCE (GCE/CuO) with powdered version of CuO is accompanied by extreme layer to layer stacking of nanostructures with incomplete and non-uniform coverage of the electrode surface area. Moreover, the use of polymeric binders further hinder the electro-catalytic performance of the modified electrode.

The charge transfer co-efficient ( $\alpha$ ) were estimated for ITO/CuO and GCE/CuO from the Tafel slopes obtained from the rising portion of the measured cyclic voltammograms (Fig. 4(b) and (c)). The estimated electron transfer co-efficient ( $\alpha$ ) for ITO/CuO was 0.83 whereas for GCE/CuO 0.73 was noted. It is clear that the estimated  $\alpha$  value for ITO/CuO is relatively higher than GCE/CuO and many other electrode system represented in Table 1. This shows the greater oxidation favorability of CAP molecules at the surface of ITO/CuO electrode.

### 3.3 The chronoamperometric measurement

The diffusion co-efficient ( $D$ ) for the electro-oxidation of CAP over ITO/CuO was estimated using chronoamperometric measurements. The chronoamperometric graph was recorded under constant pre-set potential of 0.39 V against the CAP concentration in range of 0.1 to 0.5 mM. In case of an electro active molecule (CAP) with diffusion co-efficient denoted as  $D$ , the current density for the electro-catalytic oxidation at ITO/CuO can be defined using the following modified Cottrell equation:<sup>21</sup>

$$I = nFAD^{1/2}C_b\pi^{-1/2}t^{-1/2} \quad (1)$$

$$D = \left( \frac{m}{nFAC_b\pi^{-\frac{1}{2}}} \right)^2 \quad (2)$$

where  $C_b$  is the bulk concentration of CAP,  $A$  is the area of electrode (ITO) where  $n$ ,  $F$  and  $\pi$  have their conventional meanings. Since, the reaction of interest is diffusion controlled, the plot of current ( $I$ ) is best fitted against time ( $t^{-1/2}$ ) for the various concentrations of CAP (Fig. 5(b)). The corresponding slopes are then plotted against the concentration of CAP standardised for chronoamperometric measurements (Fig. 5(c)). The final slope value was then used to estimate  $D$

value using eqn (2). In this case, the diffusion co-efficient value for ITO/CuO was estimated to be  $9.28 \times 10^{-5} \text{ cm}^2 \text{ s}^{-1}$  which is relatively higher compared to the electrodes modified using the conventional drop casting method (Table 1).

The rate constant ( $k$ ) for the CAP electro-oxidation at ITO/CuO was also deduced from the chronoamperometry data using the following Galus equation:

$$\frac{I_c}{I_L} = \gamma^{1/2} \left[ \pi^{1/2} \operatorname{erf}(\gamma^{1/2}) + \frac{\exp(-\gamma)}{\gamma^{1/2}} \right] \quad (3)$$

The  $I_c$  can be defined as the catalytic current at ITO/CuO for electro-oxidation of CAP whereas  $I_L$  is the limiting current observed in the absence of CAP. The right hand side of eqn (3) is the argument for error function. In cases where the  $\gamma$  exceeds the value of two, the error function becomes unity and thus, the eqn (3) can be simplified as eqn (4). The symbols  $k_h$ ,  $C_b$  and  $t$  represents the catalytic rate constant, bulk concentration of CAP and elapsed time respectively.

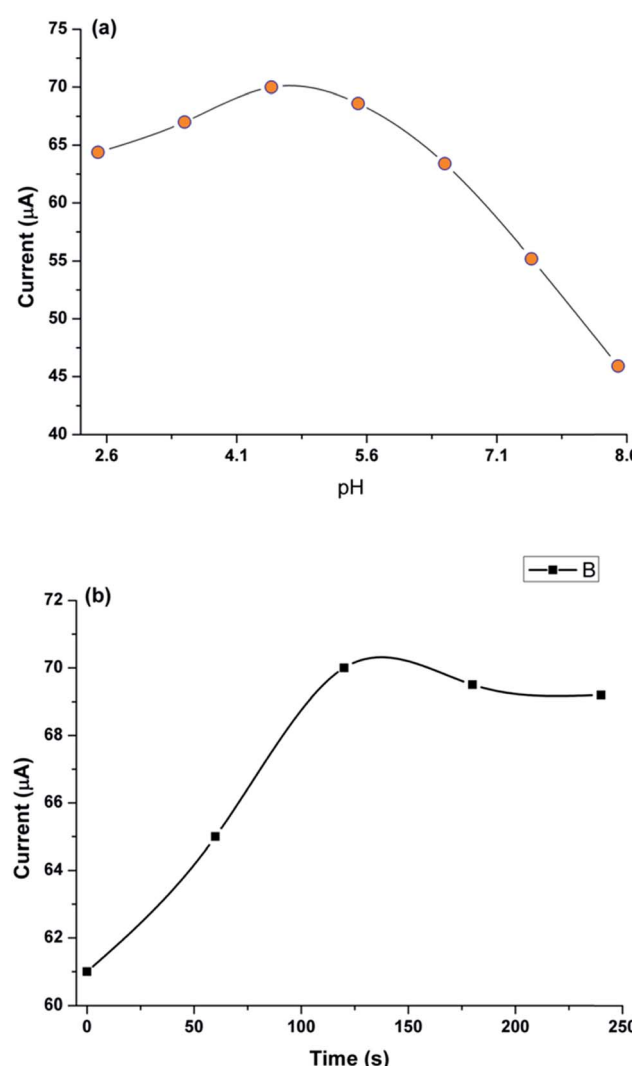


Fig. 6 Current response of ITO/CuO against (a) pH of BRB buffer and (b) accumulation time in range of 0 to 250 s.



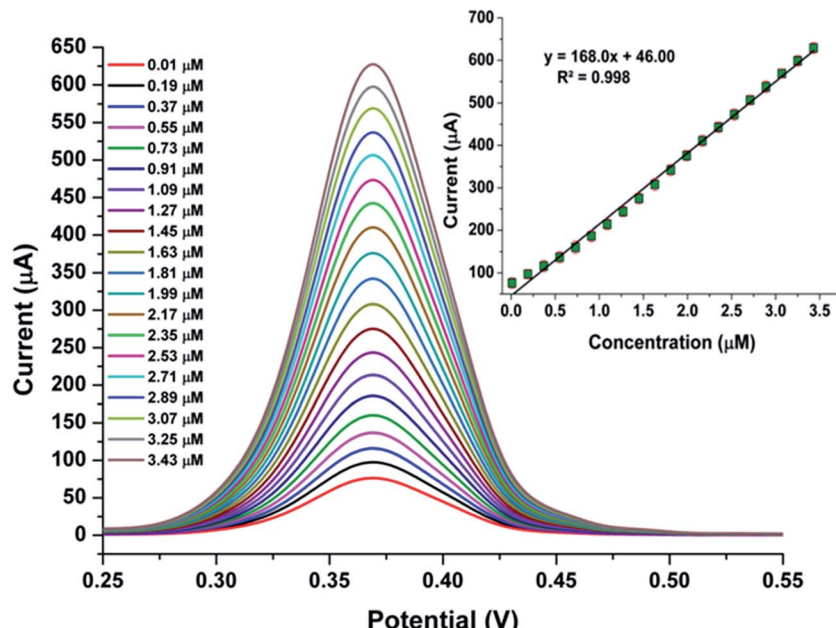


Fig. 7 DPV response of ITO/CuO against concentration of CAP in range of 0.01 to 3.43  $\mu\text{M}$  within 0.1 M BRB (pH 4.5) with corresponding calibration plot and linear fit analysis shown as inset figure.

$$\frac{I_c}{I_L} = \gamma^{1/2} \pi^{1/2} = \pi^{\frac{1}{2}} (k_h C_b t)^{1/2} \quad (4)$$

The value of  $k_h$  was estimated from the slope values of the graph plotted between  $I_c/I_L$  and  $t^{1/2}$  for the given concentration of CAP as shown in Fig. S3.† The average value of  $k_h$  was calculated to be  $3.5 \times 10^3 \text{ mol}^{-1} \text{ L s}^{-1}$ . The estimated  $k_h$  value is in complete correspondence to the well-defined anodic peak observed for the electro-catalytic oxidation of CAP over ITO/CuO electrode.

#### 3.4 The optimisation of ITO/CuO electrode

To achieve the best possible current response, the pH, scan rate and accumulation time was optimised for ITO/CuO electrode. Fig. 6(a) shows the variation in current response for ITO/CuO against pH of the solution maintained in the range of 2.5 to 8.5 against a fixed concentration of CAP (0.1  $\mu\text{M}$ ). The observed trend shows a gradual rise in the current response with an initial increase of pH from 2.5 up to 4.5 whereby the observed current density started to decline steadily. Thus, the pH 4.5 was considered optimum for electro-catalytic oxidation of CAP using ITO/CuO electrode. The variation of current density with pH of solution might be associated with the deprotonization of CAP which could affect its accumulation at the surface of ITO/CuO electrode.<sup>22</sup> The variation of anodic peak current was also studied against the scan rate in range of 50 to 90  $\text{mV s}^{-1}$  (Fig. S4†). The inset graph depicts the linear relationship between the current density and square root of scan rate suggesting the observed electro-catalytic process to be diffusion controlled. Fig. 6(b) shows the variation of anodic peak current density against the accumulation time in range of 0–250 s. The curve exhibits a gradual rise of peak current up to 100 s, thereby

transforming into a plateau which signifies the surface saturation of ITO/CuO with CAP molecules.

#### 3.5 The analytical applicability of the developed electrode

To ensure the validity of the proposed new sensor system, analytical parameters such as limit of detection (LOD), limit of quantification (LOQ) and linear working range were determined for ITO/CuO electrode. The differential pulse voltammetry (DPV) measurement were recorded for ITO/CuO against various concentrations of CAP in range of 0.01 to 3.43  $\mu\text{M}$  within 0.1 M BRB (pH 4.5). Fig. 7 shows the recorded DPV profile with inset graph exhibiting the corresponding calibration curve and linear fit analysis. The LOD and LOQ were estimated to 0.002 ( $\text{S/N} = 3$ ) and 0.08  $\mu\text{M}$  respectively. Table 1 compares the observed analytical measures of the developed sensor with those reported for the determination of CAP using conventional electrode systems. As seen, the developed sensor system demonstrates satisfactory LOD values with enhanced electrode kinetic characteristics in comparison to its conventional contenders.

#### 3.6 The interference and stability of the developed electrode

To ascertain the analytical capability of the developed electrode, the ITO/CuO was evaluated for its anti-interference potential against the common co-existing species which might interfere with the CAP analysis. The measurement was carried for various ions and molecules including  $\text{K}^+$ ,  $\text{Mg}^{2+}$ ,  $\text{Al}^{3+}$ ,  $\text{Ca}^{2+}$ ,  $\text{Fe}^{3+}$ ,  $\text{SO}_4^{2-}$ ,  $\text{CO}_3^{2-}$ ,  $\text{NO}_3^-$ , glucose, uric acid, L-cysteine, glycine, folic acid and vitamin C with concentration ten folds higher than CAP (0.1  $\mu\text{M}$ ).

The developed DPV profile (Fig. 8(a)) shows negligible variation in the anodic peak current and the potential value observed for the electrochemical oxidation of CAP using ITO/CuO. Thus, portraying the excellent anti-interference



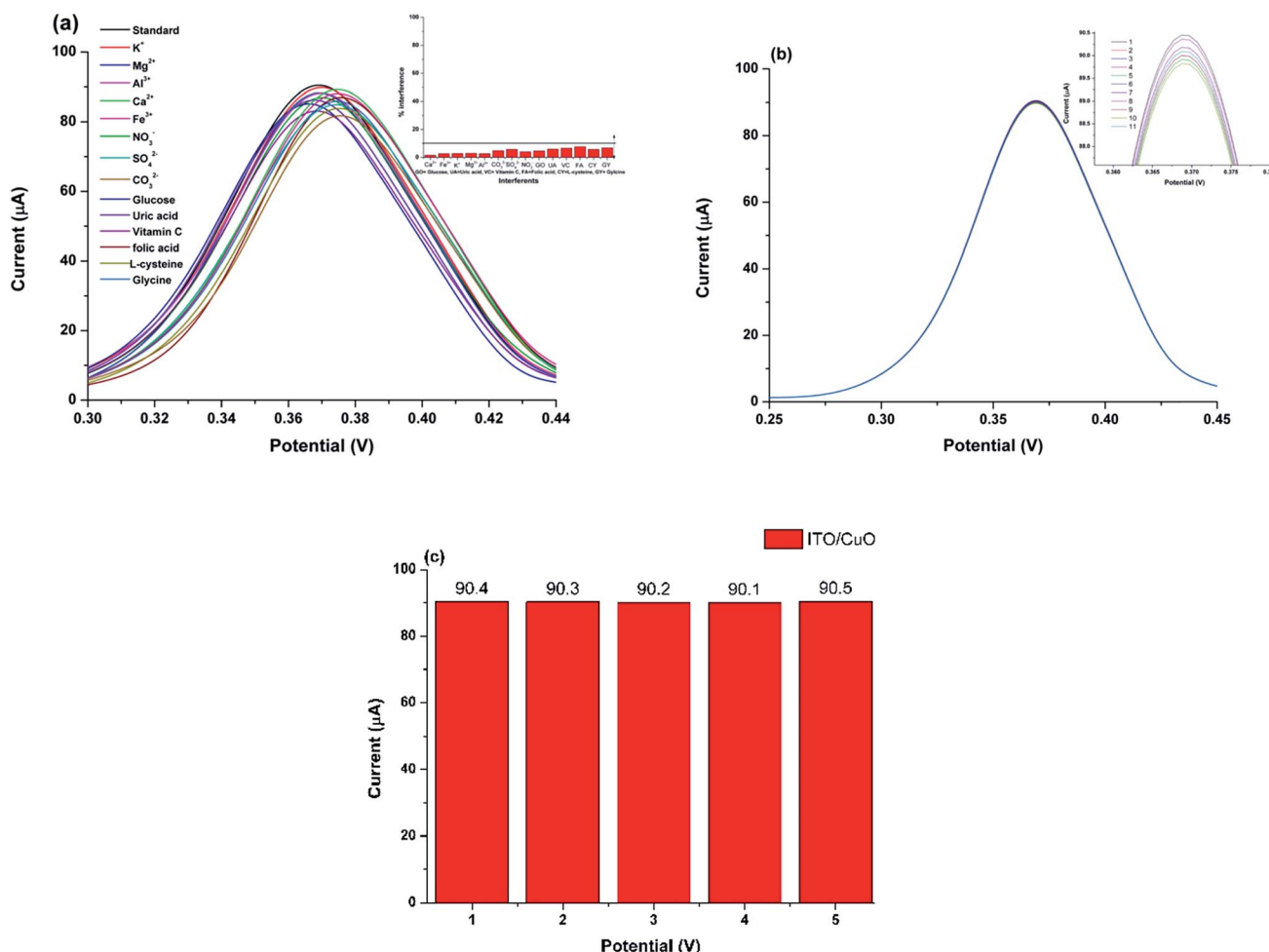


Fig. 8 (a) DPV response of ITO/CuO against common interferents with concentration ten times higher than CAP (0.1 μM) (b) cycles of DPV profile recorded for 0.1 μM of CAP to ensure working stability of the electrode and (c) variation in current density recorded for five similarly modified ITO/CuO against 0.1 μM CAP.

capability of the proposed electrode based sensor. The excellent selectivity may be attributed to the low oxidation potential window (0.39 V) for CAP at ITO/CuO which might not be sufficient for the electro-oxidation of other co-existing molecules.

The stability of the devised electrode was estimated from the relative standard deviation (RSD%) calculated for the ten successive runs of ITO/CuO within 0.1 μM of CAP in 0.1 M BR-buffer pH (4.5). The measured DPV signal variation with RSD value of <2.0% is evident of the characteristic electrode stability (Fig. 8(b)). To ascertain reproducibility in the response of the devised electrode, five ITO/CuO electrodes were separately fabricated using the exact same method described in Section 2.2. The fabricated electrode were then tested for 0.1 μM of CAP in 0.1 M BR-buffer pH (4.5). The trivial variation in the measured current response with RSD value of 1.3% signifies the excellent reproducibility of the fabricated electrode (Fig. 8(c)). Unlike, the conventional modification approaches where the random distribution of nanostructures over GCE results in very high signal fluctuation. The *in situ* growth of CuO nanostructures over flexible substrate provides a promising alternative to achieve regular nanostructure distribution, excellent

surface linkages and identical surface morphology for identical surface-analyte interactions. Thus, ensuring high signal reproducibility every time a new electrode is constructed.

### 3.7 Analysis of real samples

To test the capability of developed electrode against real sample environment. The ITO/CuO was used to quantify CAP from commercial tablets and human urine samples. The obtained

Table 2 The application of ITO/CUO electrode for the determination of CAP from tablet and urine samples

Sample	Added (μM)	Found (μM)	RSD (%)	Recovery (%)
Tablet <sup>a</sup>	0	0.098 ± 0.002	2.0	98
Urine	0.25	0.24 ± 0.005	2.1	96
Urine	0.15	0.14 ± 0.001	0.7	93

<sup>a</sup> 25 mg tablet was grounded and diluted in 0.1 M BRB solution to obtain 0.1 μM CAP solution.



urine samples were spiked with specific concentration of CAP and analysed using protocol mentioned in Section 2.3. Table 2 shows the obtain recoveries for CAP from the selected samples. The excellent recoveries with low RSD values demonstrates the practical applicability of the developed electrode.

## 4. Conclusion

The present study describes the potential application of ITO based electrode in the electrochemical oxidation of captopril (CAP) drug. The newly developed electrode relies on the *in situ* grown layer of CuO nanostructure produced using simple hydrothermal route with the application of malonic acid as an effective template. The *in situ* grown CuO layer accommodates controlled population of CuO nanostructures which were found significantly active towards the electro-catalytic oxidation of captopril drug. The sensor system exhibited excellent working linearity against the CAP concentration in range of 0.001 to 4.3  $\mu\text{M}$  with LOD value down to  $2 \times 10^{-3} \mu\text{M}$ . Moreover, the high electron transfer coefficient (0.83), diffusion co-efficient ( $9.28 \times 10^{-5} \text{ cm}^2 \text{ s}^{-1}$ ) and catalytic rate constant ( $3.5 \times 10^3 \text{ mol}^{-1} \text{ L s}^{-1}$ ) supported the high electron transfer kinetics observed CAP over the surface of ITO/CuO electrode. The excellent workability of the ITO/CuO electrode against the quantification of CAP from the commercial tablets and human urine samples further proved its practical feasibility for the clinical and environmental studies.

## Acknowledgements

The authors would like to acknowledge the research facilities provided by the National center of excellence in analytical chemistry (NCEAC), Jamshoro, Pakistan.

## References

- 1 M. Mazloum-Ardakani, M. A. Sheikh-Mohseni, H. Beitollahi, A. Benvidi and H. Naeimi, Electrochemical determination of vitamin C in the presence of uric acid by a novel  $\text{TiO}_2$  nanoparticles modified carbon paste electrode, *Chin. Chem. Lett.*, 2010, **21**, 1471–1474.
- 2 Z. Taleat, M. Mazloum Ardakani, H. Naeimi, H. Beitollahi, M. Nejati and H. Reza Zare, Electrochemical behavior of ascorbic acid at a 2,2'-[3,6-dioxa-1,8-octanediylbis(nitroethylidyne)]-bis-hydroquinone carbon paste electrode, *Anal. Sci.*, 2008, **24**, 1039–1044.
- 3 H. Beitollahi, M. A. Taher, M. Ahmadipour and R. Hosseinzadeh, Electrocatalytic determination of captopril using a modified carbon nanotube paste electrode: application to determination of captopril in pharmaceutical and biological samples, *Measurement*, 2014, **47**, 770–776.
- 4 S. Mohammadi, H. Beitollahi and A. Mohadesi, Electrochemical behaviour of a modified carbon nanotube paste electrode and its application for simultaneous determination of epinephrine, uric acid and folic acid, *Sens. Lett.*, 2013, **11**, 388–394.
- 5 L. Tian and B. Liu, Fabrication of CuO nanosheets modified Cu electrode and its excellent electrocatalytic performance towards glucose, *Appl. Surf. Sci.*, 2013, **283**, 947–953.
- 6 H. Karimi-Maleh, A. A. Ensaifi, H. Beitollahi, V. Nasiri, M. A. Khalilzadeh and P. Biparva, Electrocatalytic determination of sulfite using a modified carbon nanotubes paste electrode: application for determination of sulfite in real samples, *Ionics*, 2012, **18**, 687–694.
- 7 R. A. Soomro, A. Nafady, K. R. Hallam, S. Jawaid, A. Al Enizi, S. T. H. Sherazi, *et al.*, Highly sensitive determination of atropine using cobalt oxide nanostructures: influence of functional groups on the signal sensitivity, *Anal. Chim. Acta*, 2016, **948**, 30–39.
- 8 M. M. Foroughi, H. Beitollahi, S. Tajik, M. Hamzavi and H. Parvan, Hydroxylamine electrochemical sensor based on a modified carbon nanotube paste electrode: application to determination of hydroxylamine in water samples, *Int. J. Electrochem. Sci.*, 2014, **9**, 2955–2965.
- 9 M. Mazloum-Ardakani, B. Ganjipour, H. Beitollahi, M. K. Amini, F. Mirkhalaf, H. Naeimi, *et al.*, Simultaneous determination of levodopa, carbidopa and tryptophan using nanostructured electrochemical sensor based on novel hydroquinone and carbon nanotubes: application to the analysis of some real samples, *Electrochim. Acta*, 2011, **56**, 9113–9120.
- 10 R. A. Soomro, O. P. Akyuz, R. Ozturk and Z. H. Ibupoto, Highly sensitive non-enzymatic glucose sensing using gold nanocages as efficient electrode material, *Sens. Actuators, B*, 2016, **233**, 230–236.
- 11 Y. Jing, X. Yuan, Q. Yuan, K. He, Y. Liu, P. Lu, *et al.*, Determination of nicotine in tobacco products based on mussel-inspired reduced graphene oxide-supported gold nanoparticles, *Sci. Rep.*, 2016, **6**, 29230.
- 12 P. Feng, S. Peng, P. Wu, C. Gao, W. Huang, Y. Deng, *et al.*, A nano-sandwich construct built with graphene nanosheets and carbon nanotubes enhances mechanical properties of hydroxyapatite–polyetheretherketone scaffolds, *Int. J. Nanomed.*, 2016, **11**, 3487–3500.
- 13 T. Wang, W. Su, Y. Fu and J. Hu, Controllably annealed CuO-nanoparticle modified ITO electrodes: characterisation and electrochemical studies, *Appl. Surf. Sci.*, 2016, **390**, 795–803.
- 14 T. D. Thanh, J. Balamurugan, J. Y. Hwang, N. H. Kim and J. H. Lee, *In situ* synthesis of graphene-encapsulated gold nanoparticle hybrid electrodes for non-enzymatic glucose sensing, *Carbon*, 2016, **98**, 90–98.
- 15 A. B. F. Vitoreti, O. Abrahão, R. Gomes, G. R. Salazar-Banda and R. T. Oliveira, Electroanalytical determination of captopril in pharmaceutical formulations using boron-doped diamond electrodes, *Int. J. Electrochem. Sci.*, 2014, **9**, 1044–1054.
- 16 H. Karimi-Maleh and M. Keyvanfar, Voltammetric determination of captopril using multiwall carbon nanotubes paste electrode in the presence of isoproterenol as a mediator, *Iran. J. Pharm. Res.*, 2016, **15**, 107–117.
- 17 M. C. C. Areias, K. Shimizu and R. G. Compton, Voltammetric detection of captopril using copper(II) and



an unmodified glassy carbon electrode, *Electroanalysis*, 2016, **28**, 1524–1529.

18 B. Zargar, H. Parham and A. Hatamie, Electrochemical investigation and stripping voltammetric determination of captopril at CuO nanoparticles/multi-wall carbon nanotube nanocomposite electrode in tablet and urine samples, *Anal. Methods*, 2015, **7**, 1026–1035.

19 T. D. Nguyen, T. C. Dang, A. T. Ta and K. A. Dao, Direct growth of CuO/ITO nanowires by the vapor solid oxidation method, *J. Mater. Sci.: Mater. Electron.*, 2016, **27**, 4410–4416.

20 A. C. Ngandjong, C. Mottet and J. Puibasset, Influence of the Silica Support on the Structure and the Morphology of Silver Nanoparticles: A Molecular Simulation Study, *J. Phys. Chem. C*, 2016, **120**, 8323–8332.

21 H. Beitollahi, M. A. Taher, F. Mirrahimi and R. Hosseinzadeh, Electrochemical sensor for selective determination of *N*-acetylcysteine in the presence of folic acid using a modified carbon nanotube paste electrode, *Mater. Sci. Eng., C*, 2013, **33**, 1078–1084.

22 H. Karimi-Maleh, M. Moazampour, V. K. Gupta and A. L. Sanati, Electrocatalytic determination of captopril in real samples using NiO nanoparticle modified (9,10-dihydro-9,10-ethanoanthracene-11,12-dicarboximido)-4-ethylbenzene-1,2-diol carbon paste electrode, *Sens. Actuators, B*, 2014, **199**, 47–53.

23 D. Habibi, A. R. Faraji and A. Gil, A highly sensitive supported manganese-based voltammetric sensor for the electrocatalytic determination of captopril, *Sens. Actuators, B*, 2013, **182**, 80–86.

24 H. Beitollahi, S. Ghofrani Ivari, R. Alizadeh and R. Hosseinzadeh, Preparation, Characterization and Electrochemical Application of ZnO-CuO Nanoplates for Voltammetric Determination of Captopril and Tryptophan Using Modified Carbon Paste Electrode, *Electroanalysis*, 2015, **27**, 1742–1749.

